Available online at www.eccomasproceedia.org
Eccomas Proceedia COMPDYN (2023) 1485-1498

ECCOMAS
Proceedia

COMPDYN 2023
9th ECCOMAS Thematic Conference on
Computational Methods in Structural Dynamics and Earthquake Engineering
M. Papadrakakis, M. Fragiadakis (eds.)
Athens, Greece, 12-14 June 2023

SINGLE AND MULTI-HAZARD ROBUSTNESS ASSESSMENT OF MULTI-STORY STEEL FRAME BUILDINGS

Florea Dinu[1,2], Calin Neagu[1], and Dan Dubina[1,2]

[1] Politehnica University Timisoara, CMMC Department
Ioan Curea 1, Timisoara, Romania
e-mail: florea.dinu@upt.ro; calin.neagu@up.ro; dan.dubina@upt.ro

[2] Romanian Academy, Timisoara Branch
Mihai Viteazul 24, Timisoara, Romania

Abstract

Enhancing resilience of built infrastructure against natural and human-made hazards is one of the main goals in our society. While resilience can have many components, two are of importance when structural systems are envisaged, i.e., the capacity to resist the hazard, or robustness (i), and the ability to recover from the hazard (ii) with affordable costs and a timely intervention. To cope with these requirements and reduce the risk to built environment, existing codes are revised in parallel with the development of new ones. At European level, this includes the development of a completely updated package of Eurocodes, e.g., the new seismic code prEN 1998-1-2 and provisions for design against accidental actions prEN 1991-1-7, which bring new/updated design rules, construction measures, and structural systems. But these updates do not encompass sufficient developments toward more resilient performance in case of multi-hazard environments. Thus, the simple increase of hazard level or strength demands, or other associated requirements, might not be enough to build the resilience.
In the study, two building archetypes are considered, one with perimeter moment frames on both transversal and longitudinal direction, and one with a system made of internal braced cores. Steel structures are first damaged by an earthquake, then are tested for a column loss located on the perimeter. For reference, same column loss scenarios are applied on the intact structures. Numerical models for beams employ concentrated hinge models, defined by parameters given in prEN 1998-1-2, and fiber hinge models, calibrated against relevant test data.

Keywords: Resilience, multi-hazard, progressive collapse, catenary action, dissipation capacity, concentrated hinge model, fiber hinge model.

ISSN:2623-3347
Peer-review under responsibility of the organizing committee of COMPDYN 2023.
doi: 10.7712/120123.10494.20855

1 INTRODUCTION

The risk from hazards is increasing worldwide, mainly as a result of urban growth cumulated with insufficient planning and urban development. Europe, with an estimated 75% of population living in urban areas, is part of this increased likelihood of disasters. Such disasters lead to disruption of vital services, and recovery may take weeks, months, or longer time. The society is relatively resistant to short emergency situations; however, it is vulnerable to long-term emergency states that often lead to a social disintegration. A strategic goal of the Hyogo Framework for Action 2005-2015: Building the resilience of nations and communities to disasters (www.unisdr.org) was "the development and strengthening of institutions, mechanisms and capacities at all levels, in particular at the community level, that can systematically contribute to building resilience to hazards".

When hazards, either natural (e.g., earthquake) or industrial (human-made) impact vulnerable and exposed systems, the results are economic and/or human losses. The consequences are even deadlier when one disaster triggers another disaster, e.g., tsunami after earthquake, or when multiple hazards occur over a period of time, e.g., fire after earthquake ([1]) or earthquake after earthquake. Two representative examples from the later are the Christchurch (New Zealand) earthquake series of 2010-2011, and 2023 Turkey-Syria earthquakes. In the first example, it was not the strongest motion (i.e., 7.1 moment magnitude Mw, 2010) to cause the most losses (economic costs, fatalities) but the smaller 2011 aftershock (6.2 Mw), which was responsible for 185 fatalities and more than 40 billion US$. So, the new earthquake models should probably include multiple individual seismic events [2]. It is also important to note that the post-earthquake reconstruction process that took place in Christchurch brought to surface the resilience as a main goal. So, even the concept was not necessarily new ([3]), it was probably the first time it was considered on such a large scale. Thus, one of the declared goals was to build "a city that will be stronger, smarter and more resilient to physical, social, and economic challenges" [4], [5]. The reconstruction favored the use of a number of innovative and emerging structural systems to make the new buildings of Christchurch more seismically resilient, e.g., low-damage/replaceable technology construction ([6]). In the second example, a series of earthquakes affected large parts of southern and central Turkey, but also northern and western Syria; this proved to be far deadlier and more costly than Christchurch events. The main earthquake, with a moment magnitude M_w 7.8 that made it the second-strongest recorded in the history of Turkey, was followed immediately by many aftershocks, including a very powerful M_w 7.7 earthquake. The death toll rose to more than 50 000 fatalities, while the cost is expected to go much beyond $100 billion. Even the reconstruction efforts were not yet started, important lessons may be drawn from this tragic event:

- More consistent design provisions towards robustness
- Improvements in engineering practice (see also "Build Back Better BBB", [7]);
- Better emergency preparedness, response, and recovery.

In terms of seismic risk, a robust structure is generally associated with a high degree of redundancy. On that purpose, the design should result in a good balance between stiffness, strength, and plastic deformation capacity of members and connections. Therefore, it is expected that, when some members are damaged, there are effective alternative routes to redistribute the loads and prevent the propagation of damage and progressive collapse. The seismic design codes in force today aim at these objectives by applying the capacity design method and relevant admissibility criteria. However, there are exceptional situations when the earthquakes are more demanding than expected, and even though structures are correctly designed, they can be at high risk. The situation can be aggravated by cascading hazards, e.g., strong seismic aftershock, explosions or localized fires after an earthquake. With safety margins exceeded and

structure going beyond Ultimate Limit State and approaching or exceeding Collapse Prevention Limit State, a partial or global collapse can be initiated [6].

In the study, two building archetypes are considered, i.e., one with perimeter moment frames on both transversal and longitudinal direction (MRF), and one with a system made of internal braced core. In the first system, the lateral loads are resisted entirely by the exterior frames, dissipating the seismic energy by ductility of the beams and connections. In this system, the interior beams are connected to the columns by shear (simple) connections and do not contribute to the lateral resistance ([8]). The beam-to-column joints of the MRFs are full-strength and rigid. In case of the second system (EBF), the lateral loads are resisted by two cores with eccentric braced frames. Additionally, perimeter frames are also used, but their contribution to the lateral resistance is neglected, and they are designed to resist gravity loads only. They are however particularly efficient in minimizing the torsional effects [9], which tend to stress the different structural elements in a non-uniform way [10], but also in increasing the structure's redundancy and protection against column loss ([9]).

Note that, according to EN1998 provisions [11], a steel frame system can be classified as dual structure with both moment resisting frames and braced frames acting in the same direction only if the moment resisting frames contribute with at least 25 % to the total plastic strength of the dual frame. If the later condition is not fulfilled, the system is not a dual structure but an eccentric braced frame system.

The case-study buildings are initially designed for the ultimate limit state (ULS) and serviceability limit state (SLS), with additional requirements for damage limitation state (DL) in case of seismic action. The development of plastic mechanisms at ULS was verified using push-over analyses [11]. The structures were tested for cascading hazard scenarios that involve a strong ground motion followed by the loss of a column located on the perimeter. In the first step, the structure is subjected to a design earthquake using response history analyses. In the second step, the structure already tested for the design earthquake is investigated for a column loss scenario using the alternative load path (ALP) method and nonlinear dynamic procedure (NDP), in accordance with the UFC 4-023-03 guidelines [12]. For reference, same column loss scenarios are applied on the intact structures using same ALP method and NDP. For perimeter beams, where large deformations are expected to occur after the loss of a column, the analysis was done using concentrated hinge models, defined using parameters given in prEN 1998-1-2 [10], but also fiber-type models calibrated against relevant test data [13].

2 GENERAL SPECIFICATIONS

First building archetype, MRF, has perimeter moment frames on both transversal and longitudinal direction (Figure 1). Note that, on X direction, the first and last span have pinned ended beams. Second building archetype, EBF, has two braced cores made from eccentric braced frames (Figure 2). Additionally, perimeter moment resisting frames are also used, but their contribution in resisting lateral loads is neglected and they are designed to resist gravity loads, only.

The structures have 5 stories of 4.0 m high each, 6 bays of 7.5 m in the X direction, and 4 bays of 7.5 m in the Y direction. The design was done using S355 steel for all beams, while braces and columns were made of S460 steel grade. Excepting the braces, which were made of circular hollow sections, H sections were used for the remaining structure. The beam-to-column joints where considered full strength and rigid [14], with additional requirements for seismic resistant systems [11]. The actions that were used in the design of each structural typology are:

- Dead load: $g_k = 5$ kN/m^2 on floors, and $g_k = 4$ kN/m on the façade
- Live load for office buildings (including roof): $q_k = 3$ kN/m^2
- Wind pressure: $q_b = 0.4$ kN/m^2

- Seismic action: Type 1 response spectrum, ground type D, a_g= 0.40g, q = 6 [11].

Combination of actions for ULS and SLS were considered in compliance with EN 1990 [15]. Additionally, according to EN 1998, structures were verified for DL requirements. 3D models and linear elastic analyses were used in design. The calculations were performed using the SAP2000 software. For the seismic design, a response spectrum analysis (RSA) was conducted. The output of the design is presented in Table 1 (MRF structure) and Table 2 (for EBF structure). Additionally, the plastic mechanism and seismic response were verified by means of nonlinear static analysis procedure (push-over analysis), see Figure 3. As may be seen from Figure 3, MRF and EBF structures have similar base shear yield strengths.

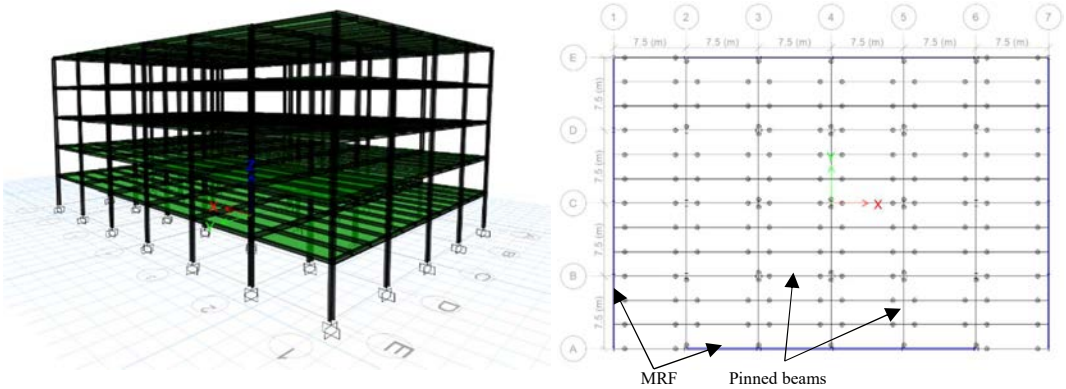

Figure 1: Geometry of the structural system, MRF: a) isometric view; b) plan view

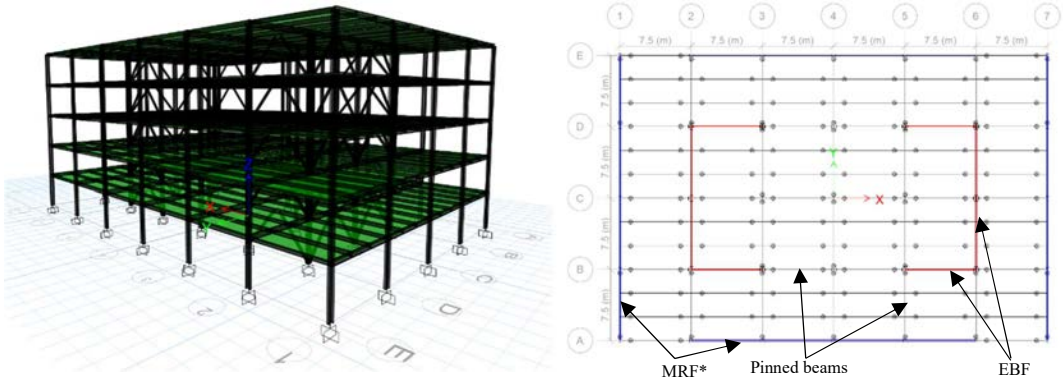

Figure 2: Geometry of the structural system, EBF: a) isometric view; b) plan view (* MRF designed for gravity loads only)

Element	Direction	Story	Section
Perimeter beams	X	1-5	IPE550*
	Y	1-5	IPE550
Interior beams	X	1-5	IPE300
	Y	1-5	IPE450
Perimeter columns	X	1-2	HE600M
		3-5	HE550M
	Y	1-2	HE650M
		3-5	HE550M
Interior columns			HE400B

** The pinned ended beams in A/E/1-2 and A/E/6-7 are made of IPE300*

Table 1: Sections for beams and columns in MRF structure

Element	Direction	Story	Section
Perimeter beams	X	1-5	IPE270*
	Y	1-5	IPE400
Interior beams	X	1-5	IPE300
	Y	1-5	IPE450
Perimeter columns	X	1-5	HE400B
	Y	1-5	HE400B
Interior columns*			HE400B
Inner braced core columns			2xHEM550
Brace	X	1-3	CHS323x14
		4-5	CHS273x10
	Y	1-3	CHS323x14
		4-5	CHS323x14

** Interior columns adjacent to pinned ended beams*

Table 2: Sections for beams, columns, and braces in EBF structure

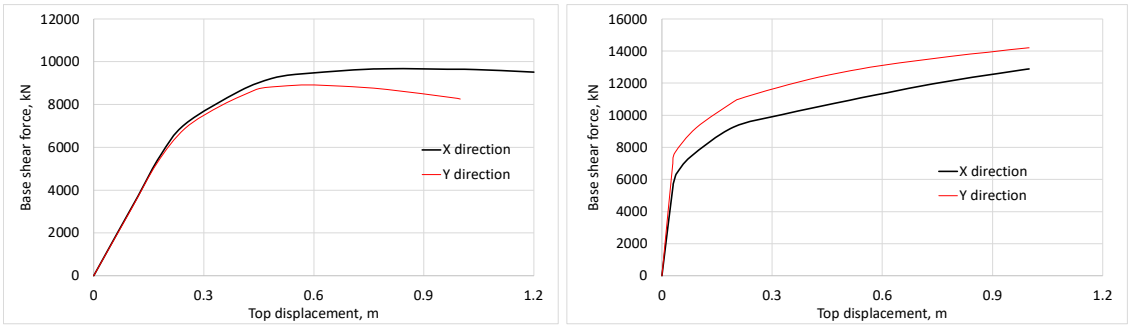

Figure 3: Capacity curves from push over analysis, X and Y direction, modal lateral load pattern: a) MRF structure; b) EBF structure

3 DEFINITION OF HAZARD SCENARIOS AND ROBUSTNESS ANALYSIS PROCEDURES

The main objective of the study is to evaluate the robustness of multi-story steel frame building structures in the aftermath of single or multi-hazard load events. The single hazard events refer to sudden loss of a column from the perimeter frames (e.g., from a localized fire or near field blast) and a strong earthquake, respectively. Lessons learned from the catastrophic series of earthquakes that struck Turkey, or the fires that followed the 1995 Kobe earthquake [1] show that the loading conditions can exceed the code provisions, and many buildings can be at high risk of severe damage or complete collapse. As a result, multi-hazard events were also considered, i.e., loss of a column from perimeter following a strong earthquake.

Column loss events, either as single hazards or following an earthquake, are investigated using the ALP method and nonlinear dynamic procedure (NDP), in accordance with the UFC 4-023-03 guidelines [12]. The ALP method ascertains the capacity of a structure to resist the loss of a critical load-bearing element without causing disproportionate collapse. Two locations are considered for column loss, both from the ground floor. First is a perimeter column from the long side (column A4) and the other is a perimeter column from the short side (column C1). Columns are assumed to be removed one at a time. As reported in [9], the loss of a column from gravity load resisting area leads in most cases to extensive failures, because the beams attached to the columns are generally connected using simple connections that are not capable of resisting the axial forces developed in the beams. Therefore, in the study, only columns from moment

resisting frames are of interest. In the NDP, first, the gravity loads are calculated with eq. (1) applied on the structure using a static analysis:

$$G = [DL + 0.5LL] \tag{1}$$

where G is the gravity load on floors, DL is the dead load and LL is the live load.

Then, in the second stage, the column is removed almost instantaneously (i.e., 0.001 seconds) to account for the dynamic effects, and the structure is analyzed using NDP.

The seismic performance of the structures is assessed using nonlinear response history analyses (RHA) considering a strong ground motion record from Northridge 1994 earthquake, i.e., Los Angeles County Fire Station record, with PGA = 5.78 m/s^2. The ground motion time history is scaled to match the target spectrum (i.e., a_g=0.4 g) using the Frequency Domain Method available in SAP2000 program.

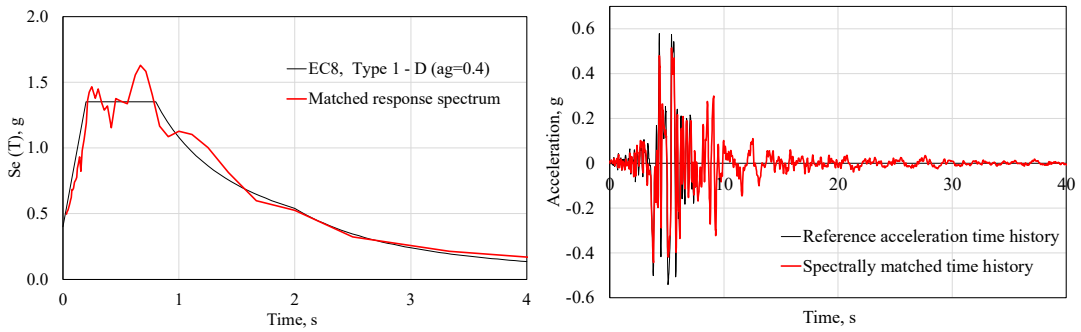

Figure 4: Ground motion used in seismic analysis: a) ground motion spectrum matched to [11] type spectrum used in design; b) reference and spectrally matched time histories

For the multi-hazard scenarios involving column loss after earthquake, the analysis procedure is done in three steps. In the first step, the structure is loaded with gravity loads assumed to be present during earthquake, which are computed using eq. (1). In the second step, the seismic response is calculated using RHA analysis applying a ground motion time history scaled to match the target spectrum. Then, in the third step, the column is removed and the NDP is applied.

For the analysis of steel moment frames, the modeling of possible nonlinear response of columns, and links and braces (for EBF only) was done using concentrated hinge models, i.e., interacting axial-flexural (P-M_2-M_3) hinges for columns, shear hinges (V_2) for links, and axial hinges (P) for braces, respectively. The modeling parameters and acceptance criteria were taken according to [16].

For perimeter beams however, the analysis was done using discrete concentrated hinge models but also fiber-type hinge models. The later models offer more accuracy than concentrated hinge models, especially for beams under axial load moment (P-M_3) interaction, which can occur at large deformation stage.

The modeling parameters and acceptance criteria for discrete concentrated hinges in beams were defined using provisions from [10] (see Figure 5), and are presented in Table 3. These parameters are based on tests data for beams under cyclic loading, and therefore they are appropriate for seismic analysis. The most influential aspects of the response are the peak rotation, θ_p, and the descending slope of the post-peak response [17]. Large monotonic-like pulses can significantly improve collapse resistance, compared to what results from more symmetric cyclic loading. For column loss analysis, UFC 4-023-03 document [12] stipulates that nonlinear procedures can adopt the modeling parameters and acceptance criteria from seismic standards (in this

case ASCE 41 [18]), even there are significant differences between the two phenomena (monotonic vs. cyclic, bending moment vs. bending moment-axial tension interaction). As a result, if for seismic analysis the capacity is taken from the backbone curve presented in Figure 5 (and Table 3), including the post-peak response if necessary, for the column loss analysis the capacity will be considered exceeded if the rotation demand is larger than θ_p, because in case of progressive collapse, the gravity loads are permanent.

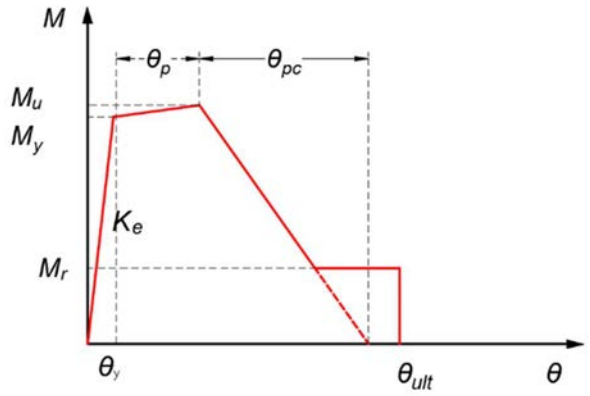

Figure 5: Moment versus hinge rotation response for steel beams [10]

Beam	M_y	M_u	θ_y	θ_p	θ_{pc}	θ_{ult}*
	kNm	kNm	mrad	mrad	mrad	mrad
IPE550	1045	1149.5	9.73	16.3	108.3	80
IPE400	490.1	539.1	13.2	22.8	115.4	80
IPE360	382.1	420.3	14.7	26.16	119	80
IPE270	181.5	199.6	19.6	40.4	131.7	80

* According to [10], this may be assumed to be 80 mrad, regardless of the full resistance beam-to-column connection type

Table 3: Modeling parameters for discrete hinges in beams

The fiber hinge parameters were calibrated using experimental data obtained on a two-way steel frame system tested under the removal of a central column [13]. The test setup is presented in Figure 6a. The beams were connected to columns with full strength and rigid joints made with extended endplate bolted connections. The vertical load was applied quasi-statically at the top of the central column using a displacement control protocol and was gradually increased until the failure of the specimen. The system could develop large deformations associated with catenary response in the beams without failure of the connections, see Figure 6b. The numerical model, with geometry, cross sections, and material properties based on tests, was built in SAP2000 software (Figure 6c). The nonlinear modeling of beams and columns was done using fiber hinge elements. The ultimate vertical load capacity of the numerical model was obtained by carrying out a displacement controlled dynamic pushdown analysis, but with a low speed, similar to the experimental one.

Figure 6d shows the vertical force versus vertical displacement curves at the central column. The numerical results show a very good correlation with the experimental ones. The results were obtained using a hinge length equal to $0.6d_b$, where d_b is the section depth. Note that the hinge length depends on loading conditions and expected level of deformation [19].

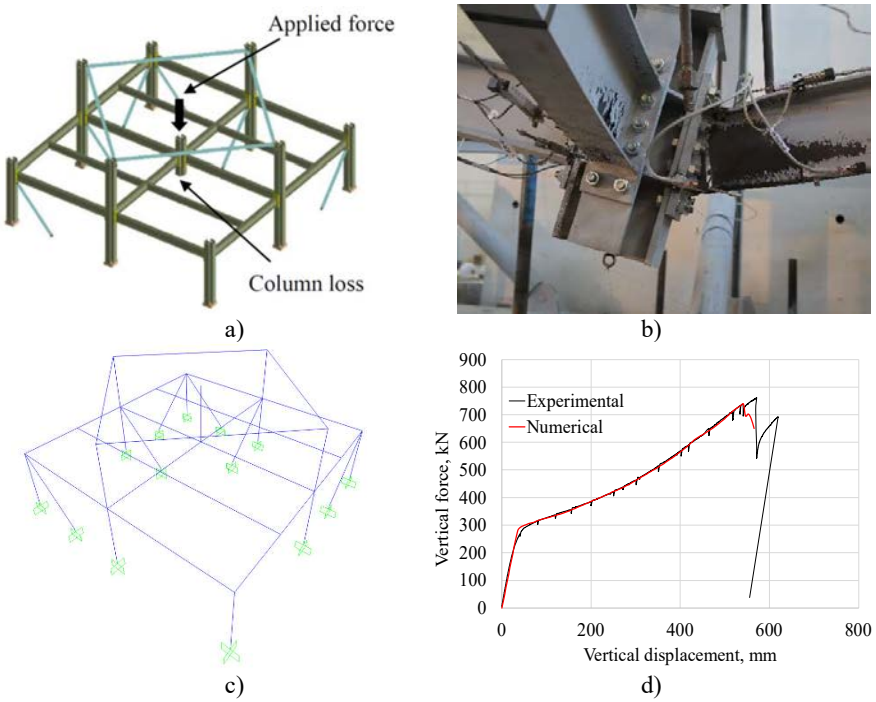

Figure 6: Experimental test used for calibration of fiber hinge model: a) test setup; b) beam failure after the development of large catenary action in beams; c) SAP2000 numerical model; d) force-displacement curves, experimental vs. numerical

4 RESULTS

The damage state in the MRF and EBF structures is first evaluated for single load events, i.e., loss of a column located on the perimeter (A4 and C1) and earthquake scaled to match the target spectrum, respectively. The two hazards are treated as independent phenomena. Then, the structure is investigated for a multi-hazard load event, with the earthquake occurring first and then the column loss. The interaction is unidirectional, and shows an increased probability relationship [20], i.e., the earthquake (and earthquake induced damages) increases the probability of a column loss.

4.1 MRF structure

Figure 7 shows the results for MRF structure. Thus, Figure 7a shows the history of vertical displacement above the lost column for column loss and column loss after earthquake, while Figure 7b shows the deformed shape and plastic mechanism for column loss after earthquake. As also presented in [9], the seismic resistant systems with perimeter moment frames are generally not vulnerable to perimeter column loss scenarios, even when the column is lost after the structure is damaged by a strong earthquake.

The vertical deflections are relatively small, and the level of maximum plastic rotation in beams is 20.4 mrad on long side frame and 21.3 mrad on short side. This is because perimeter frames concentrate most of the lateral strength and stiffness of the structure, and the resulting beams have much larger sections than required for resisting gravity loads, with utilization ratios at ULS less than 0.5.

Results also show that the acceptance criteria adopted for seismic design are generally not exceeded, and do not need to account for possible development of catenary action and large deformation response.

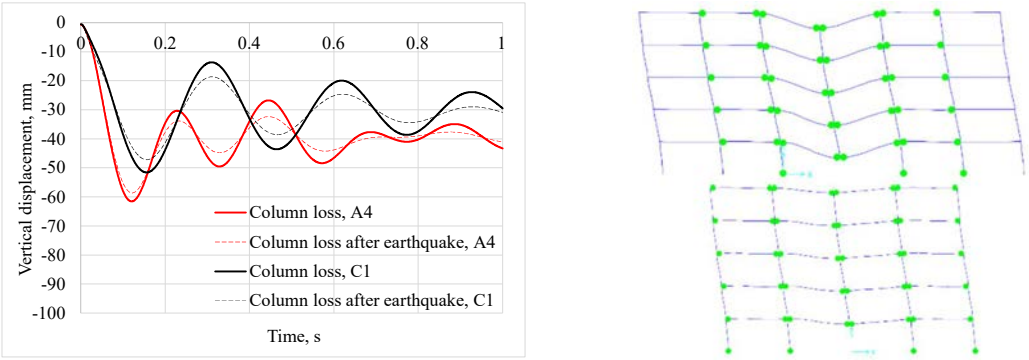

Figure 7: MRF structure: a) vertical displacement vs time for column loss and column loss after earthquake scenarios; b) deformed shape and plastic mechanism in column loss after earthquake, long side (top) and short side (bottom)

4.2 EBF structure

The second structure tested in the study is EBF, which has a lateral load resisting system made of internal braced cores and perimeter moment frames. However, the perimeter moment frames are designed to resist only gravity loads resulting from the tributary areas, and their contribution in resisting lateral loads is neglected, at least for the seismic design situation. Thus, as seen in Figure 8, the perimeter moment resisting frames contribute with less than 25 % to the total plastic stage capacity of the structure and cannot be classified as dual structures [11]. The use of perimeter moment frames instead of simple shear connections may however improve the robustness when a perimeter column is lost, as indicated in [9].

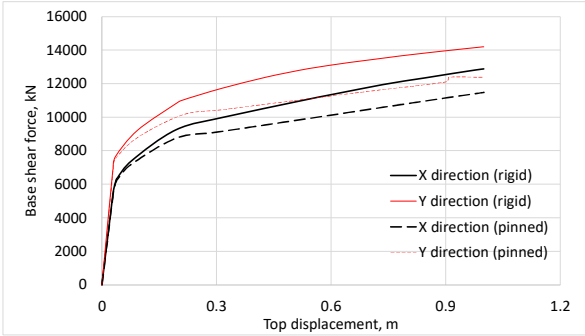

Figure 8: Capacity curves from push over analysis, X and Y direction, modal lateral load pattern, EBF structure with perimeter moment frames (rigid) and pinned ended perimeter beams (pinned)

Figure 9 shows the results for EBF structure. As seen from Figure 9a, the structure resists the seismic action primarily by the EBFs, with plastic hinges developed in all links. Few beams from 1st and 2nd stories also yield, but the maximum plastic rotations are small, i.e., 2.5 mrad on grid line 1 and 3.3 mrad on grid line A. However, as seen from Figure 9b, the structure is vulnerable to column loss scenarios on long side (grid line A), even from a single event, with deformation capacity exceeding the acceptance criteria for all beam ends away from the column loss A4 (Figure 9c). The capacity is not however exceeded in the short side perimeter frame (column loss C1), due to larger beam sections necessary to sustain gravity loads (Figure 9d). The dashed lines in Figure 9d after the peak vertical displacement for grid line A indicate progressive collapse may be initiated due to the multiple failures of beam ends.

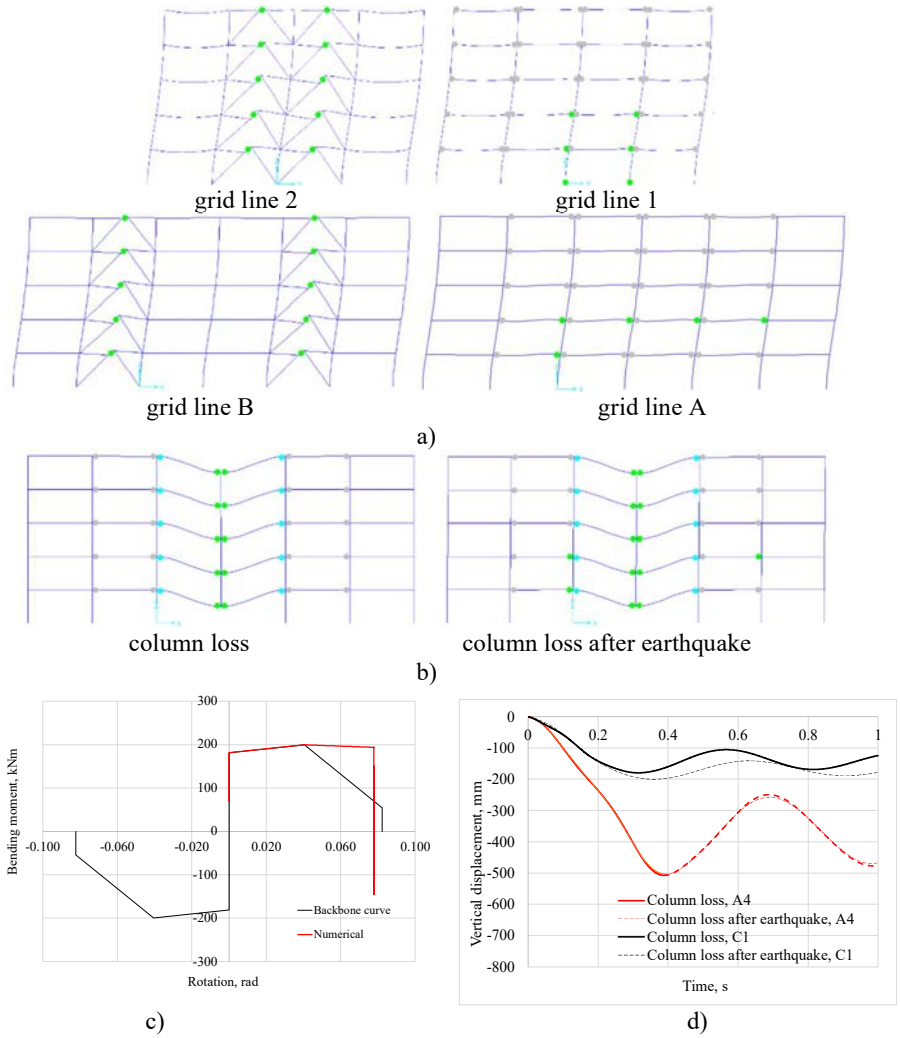

Figure 9: EBF structure: a) deformed shape and plastic mechanism for earthquake; b) deformed shape and plastic mechanism for column loss and column loss after earthquake scenarios, grid line A; c) numerical curve vs. backbone curve for column loss in the most loaded beam, column line A; d) vertical displacement vs time

As seen, the EBF structure is vulnerable to perimeter column loss scenarios, because the structure does not have adequate flexural resistance to bridge over the missing column. In order to improve the progressive collapse resistance, first solution is to increase the flexural strength of the beams. The structure will be further denoted as EBF-F. Beam to column connections should be also capable of resisting the forces associated with the bending moments in the event of column loss. Alternatively, the beams should be designed to accommodate large deformations without fracture, which can activate the catenary action in beams. The structure will be further denoted as EBF-CA. For this second approach to be effective, beam-to-column connections must be designed to withstand large axial forces that develop at catenary stage [21]. One note that modeling parameters and acceptance criteria proposed in [10] account for flexural response of the beams, only.

For the first redesign approach, the long side perimeter beams were increased from IPE270 to IPE360, while the short side perimeter beams remained unchanged. Note that, this is the maximum cross section that can be used in long side perimeter frames without considering the

system as dual structure [11]. The modeling parameters and acceptance criteria for IPE360 beams are given in Table 3 and Figure 5. Figure 10 shows the results obtained for EBF-F structure. The structure does not meet the criteria for column loss scenario, and implicitly for column loss after earthquake scenario. Thus, the plastic mechanism is almost entirely limited to the directly affected zone (Figure 10a), but maximum ratio of the beam rotation demand to capacity is exceeded, even from a standalone event, for all beam ends away from the column loss, $\theta_u/\theta_p = 1.53$, see Figure 10b.

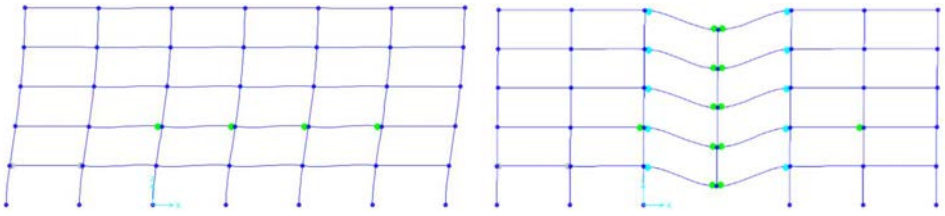

a)

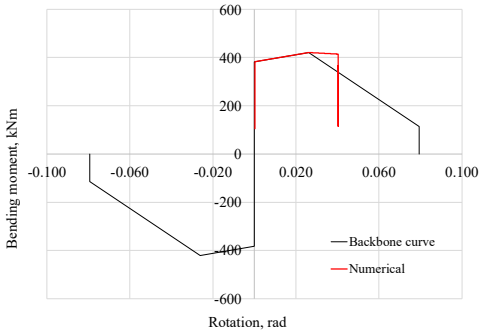

b)

Figure 10: EBF-F structure: a) plastic mechanism for earthquake (left) and column loss after earthquake (right) scenarios, long side frame; b) numerical curve vs. backbone curve for column loss in the most loaded beam, column A4

In the second redesign approach, IPE270 beams remained unchanged, but the nonlinear model was changed from concentrated hinge to fiber type hinge. The behavior of fiber hinges was calibrated against test data presented in [13] (see Section 3). Also, the beam-to-column connections were assumed to be capable of resisting the forces associated with the catenary stage (see [13]). Figure 11 shows the deformed shape and plastic mechanism for earthquake scenario and column loss after earthquake scenario. The maximum vertical displacement in the second scenario is 554 mm. In the earthquake scenario, the beam plastic rotations are small (see Figure 12a), with plastic strains in the extreme fibers limited to 0.3 %.

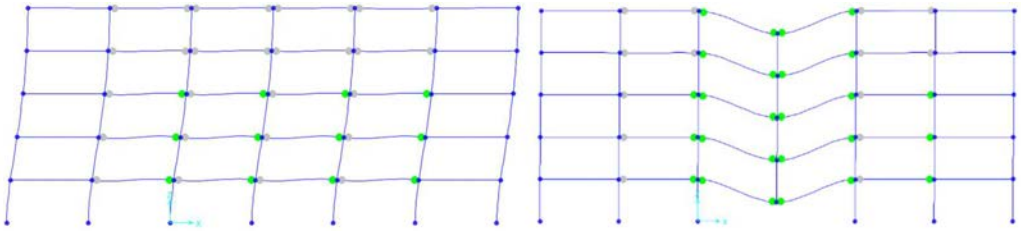

a) b)

Figure 11: Deformed shape and plastic mechanism for EBF-CA structure, long side frame: a) earthquake scenario; b) column loss after earthquake scenario

The rotation reaches 90 mrad when the column is lost after the earthquake, and the corresponding maximum strains in the most extreme fiber are 8.2 % (Figure 12b). As seen from Figure 12c, at the end of earthquake event, the residual bending moment in beam is 71.0 kNm (see also Figure 12a), and axial force is zero. After the column is lost, the axial force in beams gradually increases, and reaches a maximum of 935 kN at the maximum vertical displacement. At this point, the bending moment is 154 kNm, reduced from the peak value of 187.4 kNm developed at 350 mm vertical displacement.

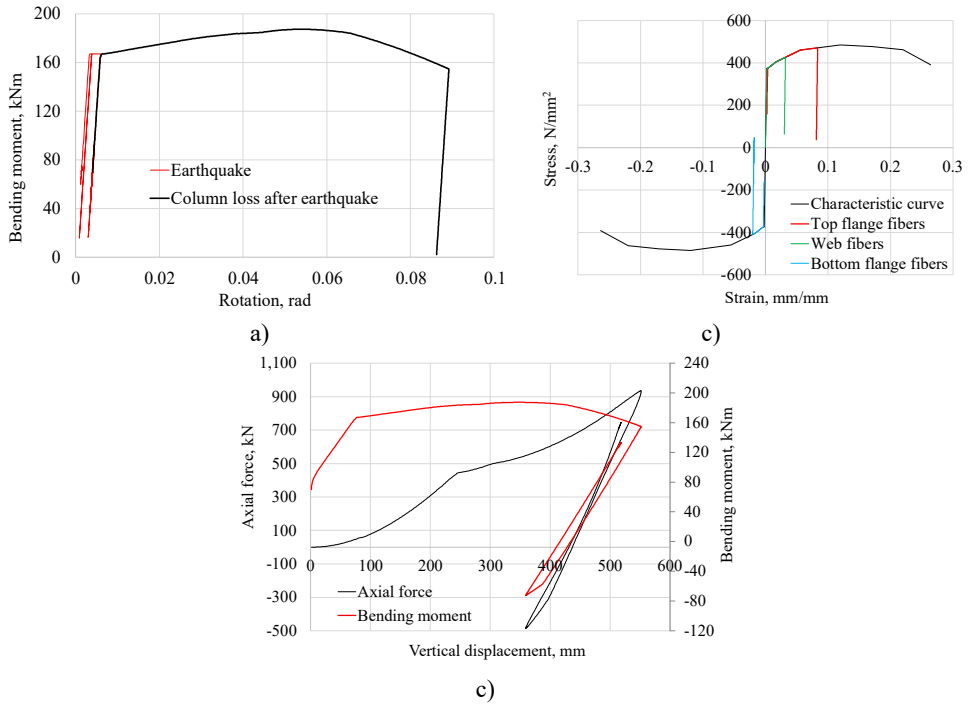

Figure 12: EBF-CA structure, 1st perimeter A4/5 beam: a) bending moment vs beam end rotation for column loss after earthquake scenario; b) fibers response vs. stress-strain curve; c) bending moment and axial force vs. vertical displacement

5 CONCLUSIONS

The study presented in the paper investigated the response of two steel frame building archetypes under a multi-hazard scenario consisting of column loss after earthquake. For reference, same column loss scenarios were applied on the intact structures. To resist seismic loads, one structure has perimeter moment frames on both transversal and longitudinal direction (MRF), and one structure has two braced cores made from eccentrically braced frames (EBF). Numerical models for beams employed concentrated hinge models, defined by parameters given in seismic standards, and fiber hinge models, calibrated against relevant test data. The structural response was evaluated using nonlinear dynamic analyses.

The results showed that perimeter frames of seismic MRF structures are not vulnerable to column loss events due to inherently large beams resulting from seismic design.

For such cases, the progressive collapse resistance is largely based on the beam flexural response. However, consideration should be given to appropriate low-cycle fatigue damage accumulation in case of large strains; alternatively, a conservative strain may be adopted. More realistic tests may be developed to reliably predict the response of beams and their end connections under multi-hazard scenarios. When the perimeter frame beams were designed from the

gravity loads only (EBF structure), they did not have sufficient flexural resistance to bridge over the missing support, due to increased gravity loads (double span conditions, dynamic effects). To avoid the increase of flexural resistance, the beams were designed to accommodate large deformations without fracture and allow the activation of the catenary action. For this approach to be effective, beam-to-column connections need to withstand large axial forces that develop at catenary stage. The fiber hinge models, calibrated against relevant test data, were used to demonstrate that the catenary action can be very effective in enhancing the collapse resistance, and thus in reducing the vulnerability in case of single or multi-hazard extreme load events.

REFERENCES

[1] "Understanding the Hazard. Fire Following Earthquake, P0181," FM Global, UK, 2015.

[2] M. Bruneau and G. MacRae, "Reconstructing Christchurch: A Seismic Shift in Building Structural Systems," p. 170.

[3] M. Bruneau *et al.*, "A Framework to Quantitatively Assess and Enhance the Seismic Resilience of Communities," *Earthquake Spectra*, vol. 19, no. 4, pp. 733–752, Nov. 2003, doi: 10.1193/1.1623497.

[4] "Community resilience." [Online]. Available: https://www.ccc.govt.nz/the-council/rebuild2011-2016/community-resilience/

[5] "Resilient Greater Christchurch." [Online]. Available: https://www.ccc.govt.nz/the-council/rebuild2011-2016/community-resilience/

[6] D. Dubina and F. Dinu, "Seismic Resilience of Multi-story Dual-Steel Building Frames," in *Progresses in European Earthquake Engineering and Seismology*, R. Vacareanu and C. Ionescu, Eds. Cham: Springer International Publishing, 2022, pp. 465–472. doi: 10.1007/978-3-031-15104-0_28.

[7] S. Mannakkara and S. Wilkinson, "Re-conceptualising 'Building Back Better' to improve post-disaster recovery," *International Journal of Managing Projects in Business*, vol. 7, no. 3, pp. 327–341, May 2014, doi: 10.1108/IJMPB-10-2013-0054.

[8] A. Astaneh-Asl, "Seismic Design of Bolted Steel Moment-Resisting Frames", Accessed: Mar. 14, 2023. [Online]. Available: https://www.academia.edu/31079812/Seismic_Design_of_Bolted_Steel_Moment_Resisting_Frames

[9] J.-F. Demonceau *et al.*, *Design Recommendations against Progressive Collapse in Steel and Steel-Concrete Buildings [FAILNOMORE]*. 2021.

[10] prEN 1998-1-2:2019.3, "Eurocode 8 - Design of structures for earthquake resistance - Part 1-2: Rules for new buildings," European Committee for Standardization, Brussels, Belgium, 2019.

[11] EN 1998-1, *Eurocode 8 - Design of structures for earthquake resistance - Part 1: General Rules, seismic actions and rules for buildings*. European Committee for Standardization, 2004.

[12] DoD, "UFC 04-023-03: Unified facilities criteria: Design of buildings to resist progressive collapse," United States Department of Defense, Washington (DC), US, UFC 04-023-03, 2009.

[13] F. Dinu, I. Marginean, D. Dubina, and I. Petran, "Experimental testing and numerical analysis of 3D steel frame system under column loss," *Engineering Structures*, vol. 113, pp. 59–70, 2016, doi: 10.1016/j.engstruct.2016.01.022.

[14] EN 1993-1-8, "Eurocode 3: Design of steel structures - Part 1-8: Design of joints," European Committee for Standardisation, Brussels, 2011.

[15] EN 1990, "Eurocode 0: Basis of Design," European Committee for Standardisation, Brussels, CEN, 2002.
[16] ASCE, *Minimum Design Loads for Buildings and Other Structures: ASCE 7-16*. Reston, UNITED STATES: American Society of Civil Engineers, 2017.
[17] D. Lignos and H. Krawinkler, "Sidesway Collapse of Deteriorating Structural Systems Under Seismic Excitations," Jul. 2012. Accessed: Mar. 23, 2023. [Online]. Available: https://purl.stanford.edu/yg701cw5473
[18] "ASCE/SEI 41-13." American Society of Civil Engineers ASCE. Seismic Rehabilitation of Existing Buildings, 2014.
[19] A. Elkady and D. G. Lignos, "Analytical investigation of the cyclic behavior and plastic hinge formation in deep wide-flange steel beam-columns," *Bull Earthquake Eng*, vol. 13, no. 4, pp. 1097–1118, Apr. 2015, doi: 10.1007/s10518-014-9640-y.
[20] J. C. Gill and B. D. Malamud, "Hazard Interactions and Interaction Networks (Cascades) within Multi-Hazard Methodologies," Management of the Earth system: integrated assessment, preprint, Jan. 2016. doi: 10.5194/esd-2015-94.
[21] B. R. Ellingwood, R. Smilowitz, D. O. Dusenberry, D. Duthinh, H. S. Lew, and N. J. Carino, "Best practices for reducing the potential for progressive collapse in buildings," National Institute of Standards and Technology, Gaithersburg, MD, NIST IR 7396, 2007. doi: 10.6028/NIST.IR.7396.